Lee *et al. Appl Biol Chem* (2019) 62:37
https://doi.org/10.1186/s13765-019-0444-2

KSABC
The Korean Society for Applied Biological Chemistry

ARTICLE Open Access

Sorption behavior of malachite green onto pristine lignin to evaluate the possibility as a dye adsorbent by lignin

Su-Lim Lee[1†], Jong-Hwan Park[2†], Seong-Heon Kim[3], Se-Won Kang[4], Ju-Sik Cho[5], Jong-Rok Jeon[1,2], Yong-Bok Lee[1,2] and Dong-Cheol Seo[1,2*]

Abstract

The objective of this study was to evaluate the adsorption characteristics of malachite green (MG) on pristine lignin as a dye adsorbent. The adsorption capacity of MG on lignin (31.2 mg/g) was described by Langmuir isotherm and pseudo second order models, and were higher than humic acid (6.4 mg/g). The adsorption of MG by lignin was rapid occurring within 15 min of the reaction, and then equilibrium was reached. The adsorption of MG by lignin based on an intraparticle diffusion model indicated that it was dominated by external boundary. Removal of MG by lignin can be applied at a wide range of pH's (2–5), and optimal lignin dosage for MG removal was 3 g/L. In addition, the desorption efficiency of MG adsorbed on lignin was highest in methanol + acetic acid (95:5%, v/v) mixture of all solutions tested. The peaks attributed to the hydrogen-bonded stretching vibrations and sulphonyl groups in lignin before MG adsorption, were assigned at about 3400 and 620 cm^{-1}, while the peaks in lignin after MG adsorption were attenuated or reduced. This result indicates that the adsorption of MG by lignin is closely related to the O–H and S–O bonds. Finally, this study suggests that pure lignin, which excludes active processes, can also be used as an adsorbent for dyes. However, in order to utilize the dye-adsorbed lignin repeatedly, further studies will be needed.

Keywords: Malachite green, Lignin, Humic acid, Adsorption, Dyes

Introduction

Recently, research into converting woody biomass into bioethanol and chemical materials has attracted much attention, and has already reached the commercialization stage [1]. In particular, the amount of lignin as a by-product of manufacturing processes increases with increasing bioethanol production, which has now reached 50 million tons per year [2]. Considering the potential for growth of the bioethanol market in future, lignin discharges are expected to increase further. Lignin is an amorphous material with an aromatic structure, which accounts for about 25–35% of woody biomass, the second most abundant natural polymeric substance after cellulose [3]. Lignin is composed of a monomer of a phenylpropane (C6-C3) structure in which a phenolic hydroxyl group and a methoxy group are bonded, and typically has a molecular structure in which three kinds of phenylpropane monomers (para-coumaryl alcohol, coniferyl alcohol and synapyl alcohol) are crosslinked [4, 5].

However, lignin is less useful due to this complicated structure, and only about 2% is used as a dispersant, an adhesive, or a surfactant, and most of the lignin produced as a by-product is discarded or incinerated [6]. Most recently, Yin et al. [7] reported that lignin has a number of functional groups including hydroxyl, methoxyl and carbonyl groups, and thus can be utilized as a raw material for chemical manufacture through chemical modification techniques such as oxypropylation and epoxidation [8]. Some researchers have found that materials derived from the chemical modification of lignin can be utilized as raw materials for making plastics such

*Correspondence: drseodc@gmail.com
†Su-Lim Lee and Jong-Hwan Park contributed equally to this work
[2] Division of Applied Life Science (BK21 Plus), Institute of Agriculture and Life Science, Gyeongsang National University, Jinju 52828, South Korea
Full list of author information is available at the end of the article

as polyurethanes and polyesters in the manufacture of plastics [9, 10], as well as raw materials for phenolic resins, epoxy resins and carbon fiber products. In terms of agriculture, lignin has a similar structure to humic acid, so that it is possible to utilize humified lignin as an agricultural fertilizer through chemical and biological modification processes [11]. However, lignin modification involves some technically demanding approaches and significant labor input, as well as coming with high costs. Furthermore, considering the daily production levels of lignin, the ability to recycle lignin by these modification methods is limited. In order to overcome these problems, there is a pressing need for a recycling method capable of large-scale application which utilizes the chemical and physical characteristics of lignin itself, without the need for modification.

As mentioned above, lignin has an aromatic three-dimensional polymer structure containing functional groups such as phenol, hydroxyl, carboxyl, methoxyl and aldehyde groups. These functional groups have been reported by many researchers to be quite effective in removing cationic contaminants including heavy metals and dyes in wastewater [12]. For example, some studies found that lignin was effective for removing heavy metals [13–15]. On the other hand, the adsorption of dyes by lignin was mostly evaluated by using activated lignin subjected to acid/alkali treatment, metal impregnation and pyrolysis [16–19]. Information about the adsorption behavior of dyes on pristine lignin however, is extremely limited. In particular, no studies have investigated the use of lignin as an adsorbent for the removal of malachite green (MG) from water.

Malachite green is a distinctive example of a basic and cationic dye, that has been widely used in medicine, fisheries, food and directly as a dye in the wood, silk, leather and paper industries. However, high concentrations of MG are toxic if discharged into the aqueous environment, with carcinogenic effects on human beings and causing suffocation of aquatic plants [20].

Therefore, the objective of this study was to evaluate the adsorption characteristics of MG by pristine lignin in order to determine whether it may be an appropriate strategy for increasing the recyclability of lignin in a way that utilize its own characteristics.

Materials and methods

Materials

Lignin, humic acid and MG were purchased from Sigma-Aldrich (Gillingham, UK). An MG stock solution was prepared at 1000 mg/L using distilled water and diluted to the concentration desired for each experiment. Solutions were adjusted to pH 5 using 0.1 M HCl or NaOH, except in the case of determining the effect of pH on MG adsorption.

Methods

Determination of the maximum adsorption capacities for MG by lignin and humic acid were performed at different initial MG concentrations. In brief, 25 mL of MG diluted solution ranging from 5 to 300 mg/L were added to a set of 100 mL glass flasks containing 0.05 g of either lignin or humic acid. After incubation with shaking for 24 h at 25 °C, the mixed samples were separated by centrifugation at 5000 rpm for 10 min. The concentrations of MG in residual solutions were analyzed by UV–Vis spectrometer (UV-1800, Shimadzu, Japan). The amount of MG adsorbed per mass unit of adsorbent was calculated by difference between the initial and equilibrium concentrations in solution. In order to determine the maximum adsorption capacity, the amount of MG adsorbed by lignin and humic acid based on initial MG concentration was applied to Freundlich and Langmuir isotherms. The equations, plots and relationship constants for the Fruendlich and Langmuir isotherms are given in Additional file 1: Table S1.

The dynamic adsorptive behavior of the adsorbent is one of the factors that must be considered for process design and operation control of the adsorption system. In this study, the dynamic adsorptive behavior was evaluated by weighing 0.05 g of lignin and humic acid in Erlenmeyer flasks (100 mL) followed by 25 mL additions of MG (50 mg/L). Samples were then equilibrated at the designated time intervals of up to 24 h. The separation and analysis of the stirred samples were carried out in the same manner as described in the isotherm experiment. To understand the adsorption mechanisms of MG by lignin and humic acid, pseudo-first-order (PFO), pseudo-second-order (PSO) and intraparticle diffusion (IPD) models were used to investigate the adsorption kinetics (Additional file 1: Table S1). In addition, the adsorption properties of MG by lignin and humic acid were evaluated at different initial pH (2–7; 50 mg/L MG) and dosage (1–4 g/L; 100 mg/L MG).

The desorption efficiency of MG-adsorbed lignin and humic acid, were evaluated in the presence of different solvents; methanol (MeOH), methanol + acetic acid (95:5%, v/v; MeOH-Ac) mixture and diluted acetic acid (5% in distilled water, v/v; Ac). MG-adsorbed samples were washed with distilled water and dried. Desorption solutions (25 mL) were added to a set of glass flasks containing 0.05 g of the MG-adsorbed sample, followed by stirring for 4 h. All analytical methods are the same as those above. The recyclability of lignin was subsequently evaluated, using the optimal desorption solution (MeOH-Ac), in desorption experiments.

Finally, we characterized the involvement of functional groups on lignin before and after MG adsorption, by Fourier transform infrared spectrometer (FTIR, Bruker VERTEX 70, Germany) in the range 400–4000 cm^{-1}, to define more precisely the chemical interactions between adsorbent and MG.

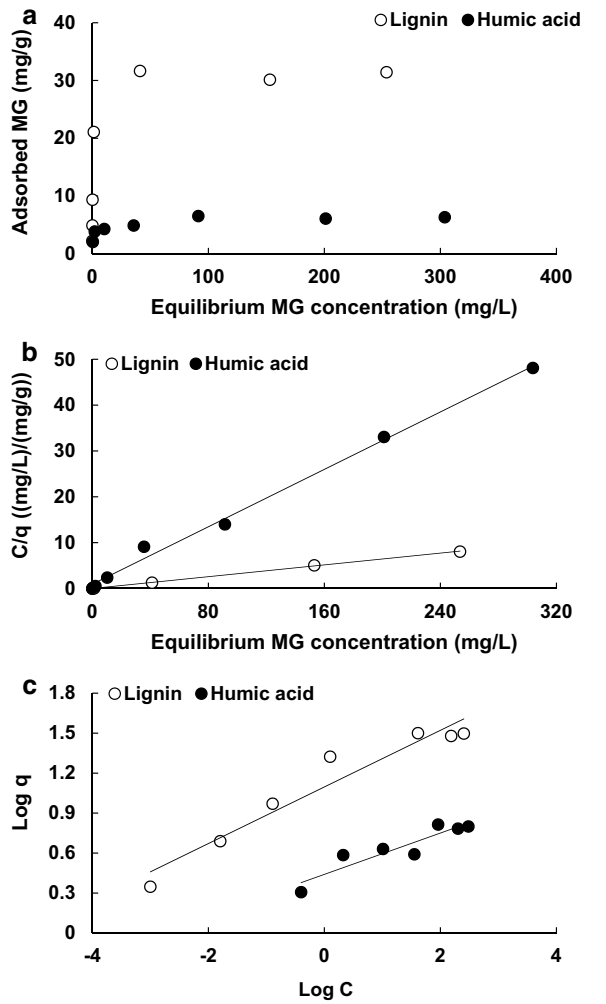

Fig. 1 Adsorption isotherm of MG by lignin and humic acid. **a** Amount of MG adsorbed by lignin and humic acid, **b** Langmuir isotherm model, and **c** Freundlich isotherm model

Results and discussion

Isotherm

The adsorption characteristics of MG by lignin and humic acid at different initial dye concentrations is shown in Fig. 1 and Table 1. As the solution concentration of MG exposed to both lignin and humic acid increased, the adsorbed amount progressively increased, whereas it reached an equilibrium at MG concentration of 100 mg/L (Fig. 1a). The amount of MG adsorbed by lignin and humic acid under these conditions was applied to Langmuir and Freundlich isotherm models. The results demonstrated that the amount of adsorbed MG was better represented by the Langmuir model (R^2 = 0.9951–0.9995) than the Freundlich model (R^2 = 0.8514–0.9349) (Fig. 1b, c. The Freundlich model assumes adsorption by active sites in heterogeneous surfaces, whereas the Langmuir model assumes adsorption by a monolayer in homogeneous surfaces [21]. Therefore, the adsorption of MG by lignin and humic acid was mechanistically dominated by monolayer adsorption to a homogeneous surface.

Of particular note, the maximum adsorption capacity (*a*) of MG by lignin was 31.2 mg/g, which was 4.9 times higher than that of humic acid (6.4 mg/g). The *b* value obtained from the Langmuir isotherm model shows the affinity between adsorbent and adsorbate, which was 2.08 for lignin and 0.17 for humic acid. These data indicate that lignin has a much higher adsorption affinity for MG than humic acid.

The maximum adsorption capacity of MG by lignin was compared to MG interactions with other adsorbents, which have previously been reported since no studies have been conducted on this specific topic.

As shown in Table 2, it is difficult to directly compare the amount of MG adsorbed by these materials, because experimental conditions, including initial MG concentration, dosage and pH used in other studies, were different. In recent times, most carbon-based byproducts have focused on the development of activated adsorbents through pyrolysis or chemical activation, and the adsorbed amounts of MG by them ranged from 12 to 435 mg/g [22–24]. The amounts of MG adsorbed by degreased coffee bean [25], oil palm trunk fiber [26] and rattan sawdust [27] were 55, 149 and 63 mg/g,

Table 1 The parameter estimates and coefficients of determination (R^2) for fit of the isotherm equation to experimental data of MG adsorption by lignin and humic acid

Materials	Freundlich adsorption isother			Langmuir adsorption isotherm		
	K	*1/n*	R^2	*a*	*b*	R^2
Lignin	12.50	0.2124	0.9349	31.2	2.08	0.9995
Humic acid	2.76	0.1549	0.8501	6.4	0.17	0.9951

Table 2 Comparison of maximum adsorption capacities of different adsorbents

Adsorbent	MAC (mg/g)	Initial pH	Dosage (g/L)	Initial MG (mg/L)	References
By-product materials					
DCB	55	4	6	25–100	Baek et al. [25]
OPTE	149	5	1.5	25–300	Hameed and El-Khaiary [26]
Rattan sawdust	63	5	1.5	25–300	Hameed and El-Khaiary [27]
Lignin	31	5	2	5–300	In this study
Synthetic materials					
Algae-AC	118	5	1	20–100	Vasanth Kumar et al. [31]
ADR-AC	9	5	6	10–100	Zhang et al. [32]
Bamboo-AC	264	NM	1	25–300	Hameed and El-Khaiary, [33]
Activated rice husk	12	7	1	10–100	Chowdhury et al. [22]
Rice husk-AC	83	5–6	1	10–100	Rahman et al. [34]
Chitosan-bentonite bead	435	6	0.28	20–60	Ngah et al. [23]
Ginger waste with $H_2SO_4 + ZnCl_2$	84	NM	1	5–20	Ahmad and Kumar [35]
Groundnut shell-AC	222	NM	0.7	5–200	Malik et al. [36]
Lignite-AC	149	natural	2	100–400	Önal et al. [37]
OMC	41	6	8	10–500	Arellano-Cárdenas et al. [24]
Natural materials					
Bentonite	179	5	10	50–300	Bulut et al. [28]
Clay soil	79	6	3	10–100	Saha et al. [29]
Zeolite	24	~4	3	20–160	Han et al. [30]
Humic acid	6	5	2	5–300	In this study

DCB degreased coffee bean, *OPTE* oil palm trunk fibre, *ADR* Arundo donax root, *OMC* organically modified clay, *NM* none measure

respectively, all of which were higher than that of lignin. Differences in amounts of MG adsorbed on these adsorbents is due to the different chemical and physical properties of the raw materials and the discharge route of byproducts.

In contrast to this underperformance by lignin, the amount of MG adsorbed by lignin was higher than that of bentonite and clay soil [28, 29], but lower than that of zeolite [30]. Based on these comparisons it appears that lignin can be used as an adsorbent for MG removal from aqueous solution, however, the performance overall was inferior to that of other adsorbents previously reported. Therefore, it appears that a new activating technique that can remove various pollutants is needed, while continuing to emphasize lignin's inherent characteristics.

Kinetics

Figure 2 shows the kinetic behavior of MG adsorption by lignin and humic acid with respect to reaction time. The amount of MG adsorbed increased rapidly up to 15 min and reached near equilibrium after 30 min (Fig. 2a). Generally, due to the abundant vacant sites in the fresh adsorbent, rapid adsorption occurs at the beginning of the reaction, and persists until the adsorption site becomes saturated [38, 39]. Our study suggests that the active sites of lignin and humic acid for MG adsorption are mostly saturated within 15 min.

The dynamic adsorption behavior of MG on lignin and humic acid was evaluated by the general kinetic models PFO (Fig. 2b) and PSO (Fig. 2c). The constants (k_1, k_2 and q_e) with correlation coefficient (R^2) obtained from these kinetic models are shown in Table 2. The adsorption of MG by lignin and humic acid was better described by the PSO model ($R^2 = 0.3403$ for humic acid and 0.6901 for lignin) than by the PFO model ($R^2 = 0.9982$ for humic acid and 1.000 for lignin), which indicate that MG adsorption by lignin and humic acid is controlled by chemosorption. This result suggested that MG adsorption by lignin and HA was a rate-limiting step and that the reaction rate is proportional to the active site numbers existing in lignin and humic acid [21, 40]. In particular, the q_e value derived from PSO of lignin was 3.2 times higher than that of humic acid, indicating that lignin had more active sites for MG adsorption than humic acid (Table 3).

The IDP model is an important factor for determining whether adsorption of adsorbate by adsorbent is due to external boundary or internal (intraparticle) diffusion [41]. When the adsorption results of MG by lignin and humic acid were applied to the IPD model, the reaction rate was divided into two stages. The first straight line represents the adsorption by the outer boundary, and the

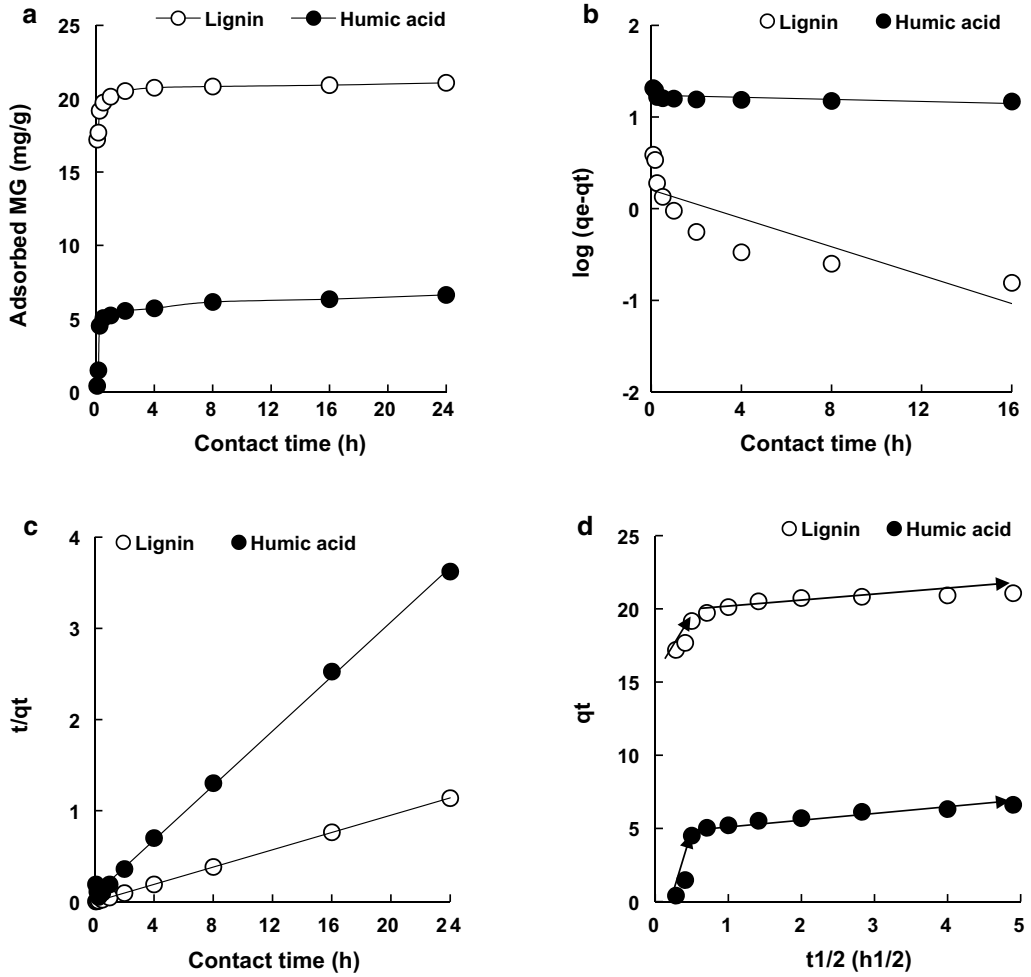

Fig. 2 Kinetics of MG by lignin and humic acid. **a** Effect of time on MG adsorption, **b** Pseudo first order model, **c** Pseudo second order model, and **d** intraparticle diffusion model

Table 3 Parameters for MG adsorption kinetics of lignin and humic acid

Kinetic models	Lignin	Humic acid
Pseudo first order		
q_e (mg/g)	1.60	17.3
k_1 (1/h)	0.178	0.013
R^2	0.6901	0.3403
Pseudo second order		
q_e (mg/g)	21.1	6.7
k_2 (g/mg/h)	1.026	0.283
R^2	1.0000	0.9982
Intraparticle diffusion		
k_i (mg/g/h$^{1/2}$)	0.3461	0.4182
C (mg/g)	19.6	4.7
R^2	0.7098	0.9064

second following line represents the adsorption by the internal diffusion model. Therefore, the results of the IPD on lignin and humic acid in this study, were derived only from the second straight line. In our study, the q_i values determined from the IPD model were 0.34 for lignin and 0.41 for humic acid, which are lower than those for carbon adsorbents such as activated charcoal and biochar [37, 42]. Therefore, adsorption of MG by lignin and humic acid is mostly dominated by external boundary.

pH effect

The adsorption characteristics of MG by lignin and humic acid based on initial pH are shown in Fig. 3. The MG standard solution (50 mg/L) was stable without any significant differences up to pH 5 (from 45.6 to 49.6 mg/L), but the absorption in UV–Vis spectrometer was reduced at higher pH values because the color of MG at the same wavelength, faded above pH 6. At pH 8, the

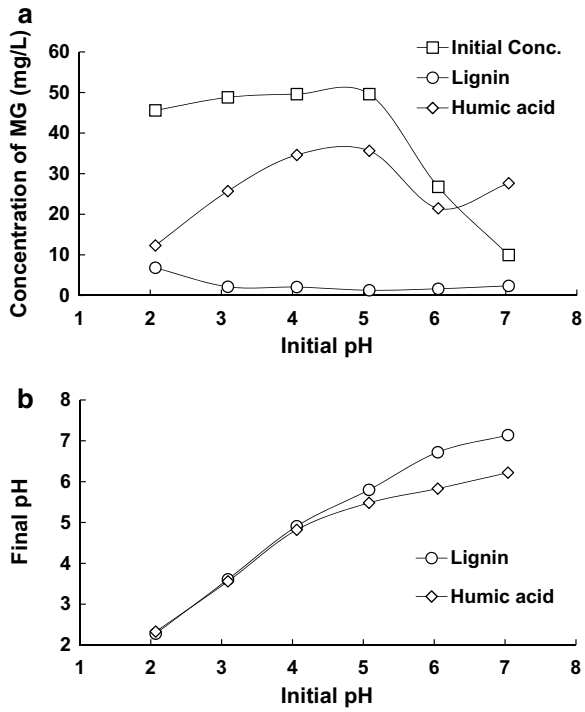

Fig. 3 Effect of pH on MG adsorption by lignin and humic acid. **a** Concentration of MG adsorbed, **b** final pH

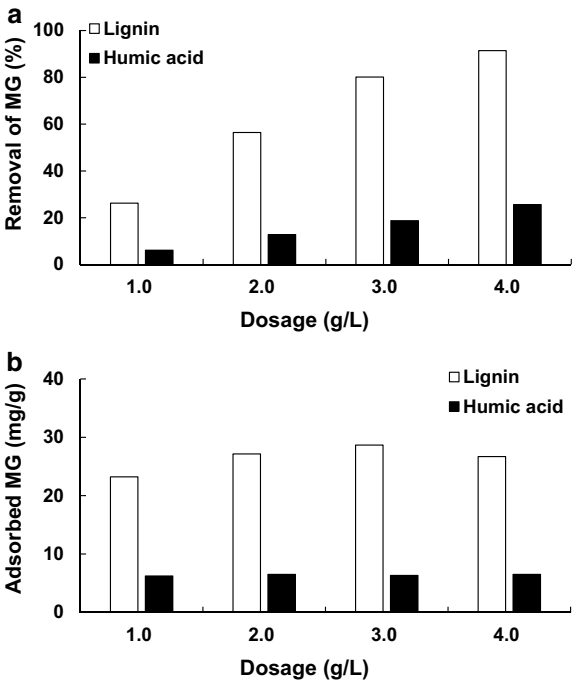

Fig. 4 Effects of lignin and humic acid dosage on MG adsorption. **a** Removal rate of MG, **b** amount of MG adsorbed

concentration of MG could not be measured because the color was completely faded. Tang et al. [18] also reported a similar result. The concentration of residual MG following adsorption by lignin was 6.8 mg/L at pH 2 but ranged between 1.3 mg/L and 2.4 mg/L for the rest of the pH value. On the other hand, when the amount of MG adsorbed by lignin was calculated based on the residual and the initial concentrations at each pH, the results showed 20.5, 23.3, 23.8, 24.2, 12.6, and 3.8 mg/g at pH 2, 3, 4, 5, 6, and 7, respectively. In order to determine the adsorbed amount of MG by lignin corresponding to the pH change, it is recommended that the pH should be adjusted to the range of 2–5.

The adsorption of MG by lignin increased with increasing pH from 2 to 5. In the acidic solution, the functional groups on the surface of the adsorbent bind H^+ and from positively charged protons. In addition, Harmita et al. [43] reported that the zeta potential charge of lignin is negative at pH 2. For these clear reasons, the adsorption of MG by lignin in the acidic state is expected to be at it's lowest rate. As the pH increases, hydrogen ion concentration in the solution reduces and MG is protonated increasing the amount of the dye adsorbed due to electrostatic attractions between lignin and MG.

In the adsorption experiment with humic acid, the adsorption capacity decreased as the pH increased from 2 to 5, a stark contrast to what was observed with lignin. Also, it appears that the adsorption capacity of MG increased at pH 6, however, this might have been due to the fading of MG standard solution. Gűrses et al. [44] reported that the increasing adsorption under acidic conditions may be related to preference of the cationic dyes for active sites and/or the increasing accessibility to interlayer regions of protonated (MGH^{2+}) and monomeric species, because of removal of some oxides at the adsorbent surface.

In particular it is worth noting that the residual MG concentration after adsorption of MG by humic acid at pH 7 was higher than the initial concentration. As shown in Fig. 3b, the final pH was lowered to less than 7 because of the pH buffering action of humic acid in solution, which is closely related to recovery of the faded color.

Dosage effect

The responses to lignin and humic acid doses are shown in Fig. 4. With increasing dosage the removal efficiency of MG increased (Fig. 4a). This is clearly due to the increasing number of active sites for adsorption. Additionally, the amount of MG adsorbed by lignin was highest at 3 g/L among all dosages tested (Fig. 4b). The increase in adsorption efficiency with dosage was more likely a function of increasing total amount of active sites [45], and our results indicate that not all of the newly available

active sites are used for MG binding. For example, with humic acid, the adsorbed amount ranged between 6.24 and 6.51 mg/g regardless of the dose, indicating that not all the increased number of active sites contributed to the adsorption of MG.

Desorption

The DW, MeOH, MeOH-Ac and diluted-Ac solutions were used to desorb lignin-adsorbed MG (Fig. 5). On a technical note, the amount of humic acid remaining after the first adsorption reaction was reduced to about 33% of the initial dose, indicating that most of it was dissolved. Therefore, experiments for desorbing on humic acid could not be carried out. The desorption efficiency of DW on the MG adsorbed-lignin was negligible. On the other hand, the desorption efficiencies of MG-adsorbed lignin by MeOH, MeOH-Ac and diluted-Ac solutions were 28.9, 78.5 and 12.3%, respectively. Hence, the desorption efficiency of MG by MeOH-Ac was dramatically higher than any of the other solutions. This result indicates that MG was adsorbed by heterogeneous adsorption site mechanisms, which likely included electrostatic attraction, hydrophobic interaction and H-bonding [46]. Of interest, Afkhami et al. [47] reported that most of the dye adsorbed on surfaces, desorbed within 2 min if there was no internal diffusion resistance to the dye inside the adsorbent. We specifically looked at this possibility and tested desorption at 2 min and 24 h. The desorption efficiency in term of the percentage of total amount adsorbed was similar regardless of desorption time (data not shown). This may be further evidence that the adsorption of MG by lignin is not affected by internal diffusion, which is in agreement with the kinetic study and IPD model mentioned.

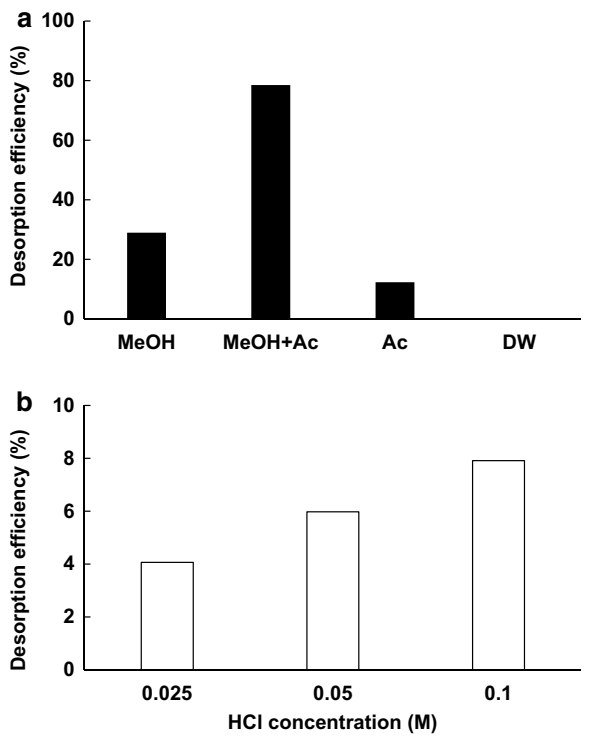

Fig. 5 Desorption characteristics of MG adsorbed on lignin under various desorption solution. **a** Methanol (Me), Me + acetic acid (AC), AC and distilled water (DW), **b** HCl

The recyclability of lignin was evaluated by initial adsorption followed by optimal desorption (MeOH-Ac). The amount of desorbed MG decreased as lignin was repeatedly re-used. However, more importantly, the amount of MG adsorbed by lignin in the second adsorption reaction was 2.3 mg/g, which was 84% lower than that of the first adsorption reaction. A reasonable explanation for these results is that the MG is not re-adsorbed following desorption because the C–OH functional groups on the lignin surface have been esterified by MeOH-Ac.

Baek et al. [25] reported that the desorption efficiency of MG adsorbed on degreased coffee bean using HCl decreased from 28.3 to 9.4% as the number of reactions increased (from 1st reaction to 3rd reaction). This study also investigated the desorption efficiency of MG adsorbed on lignin by varying HCl concentration. As the concentration of HCl increased, the desorption efficiency increased, but the amount of MG desorbed by 0.1 M HCl was approximately 2.3 mg/g, which was minimal as compared with the total adsorbed MG. The desorption efficiency of MG adsorbed on lignin under the same desorption solution (0.1 M HCl) was lower than that of the coffee bean, indicating that lignin has a higher affinity for MG than coffee bean.

Reversibility of adsorption is determined by whether there is strong bonding (ionic or/and covalent bond) or weak bonding (like Van der Waals' forces or/and dipole–dipole interaction) between the adsorbent surface and the dye molecule [48]. Based on our results, it is apparent that the bonds between lignin and MG are strong and therefore difficult to desorb by any solution.

Functional group variation in lignin before and after MG adsorption

The FTIR spectra for lignin before and after MG adsorption are shown in Fig. 6. The peaks attributed to the hydrogen-bonded stretching vibrations in the lignin before MG adsorption were broadly assigned at about 3400 cm^{-1} [49], while the peaks in lignin after MG adsorption were attenuated or reduced.

In general, the peaks represented at 620 cm^{-1} in lignin were reported to be related to the sulphonic groups [50].

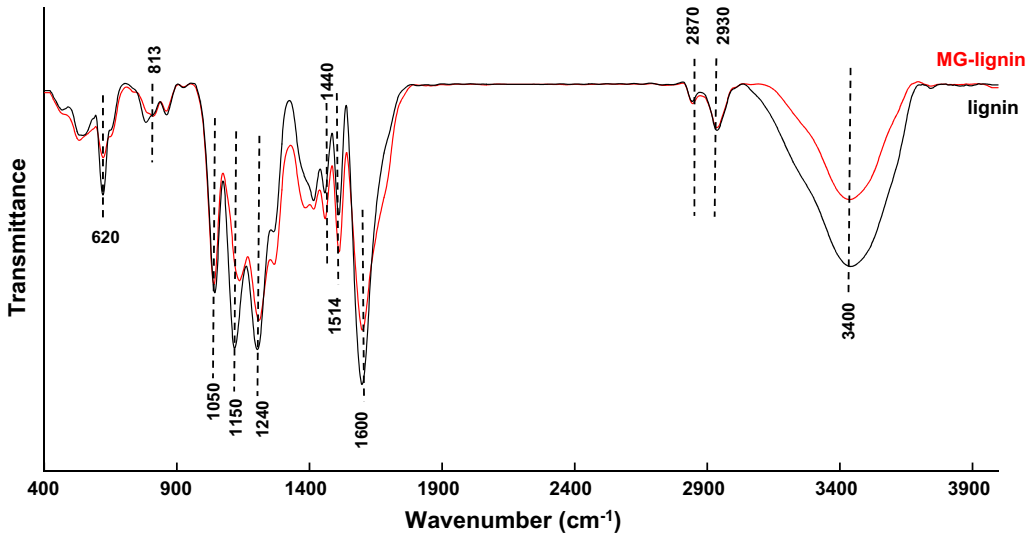

Fig. 6 Relative change in FTIR wave number identification of lignin before and after MG adsorption

This peak decreased after MG adsorption, indicating that the sulphonic (S–O) groups also contributed to MG adsorption. In support, Bekçi et al. [51] also reported that adsorption of MG by marine alga (*Caulerpa racemosa var. cylinracea*) is closely related to the sulphonic group.

Peaks were observed at 794, 1050, 1150, 1240, 1440, 1514, 1600, 2870 and 2930 cm^{-1} in lignin before MG adsorption, which were attributable to aromatic C–H stretching, symmetric C–O stretching, asymmetric C–O stretching, O–H bending, aromatic C=C stretching, secondary aromatic amines, aromatic vibration, symmetric C–H stretching and asymmetric C–H stretching, respectively [52–54]. The peak assigned at 794 cm^{-1} in lignin before MG adsorption shifted to 813 cm^{-1} after adsorption, suggesting that the aromatic group on lignin surface was increased due to adsorption of MG. The peaks assigned to 1050, 1440, 2870 and 2930 cm^{-1} in lignin were similar before and after MG adsorption. The peak related to secondary aromatic amines in lignin after MG adsorption was strongly assigned at 1514 cm^{-1}, which is attributed to MG adsorption.

Additional file

Additional file 1. Table S1. Equations, plots, and constants for adsorption isotherm and kinetic models.

Acknowledgements
This work was supported by the National Research Foundation of Korea (NRF) grant funded by the Korea Government (MSIP), [NRF-2017R1A2B4004635; NRF-2019R1C1C1004572]. This study was carried out with the support of "R&D Program for Forest Science Technology (2017041B10-1919-BA01)" provided by Korea Forest Service (Korea Forestry Promotion Institute).

Authors' contributions
S-LL, J-HP and D-CS designed and conducted the experiment as well as wrote the manuscript. S-HK and S-WK conducted FTIR analysis and interpretation. J-SC, J-RJ and Y-BL inspired the overall work and revised the final manuscript. All authors read and approved the final manuscript.

Funding
Not applicable.

Availability of data and materials
All data is available in the main text.

Competing interests
The authors declare that they have no competing interests.

Author details
[1] Department of Agricultural Chemistry and Food Science and Technology, Gyeongsang National University, Jinju 52828, South Korea. [2] Division of Applied Life Science (BK21 Plus), Institute of Agriculture and Life Science, Gyeongsang National University, Jinju 52828, South Korea. [3] Soil and Fertilizer Division, National Institute of Agricultural Sciences, Wanju 55365, South Korea. [4] Red River Research Station, Louisiana State University Agricultural Center, Bossier City, LA 71112, USA. [5] Department of Bio-Environmental Sciences, Sunchon National University, Suncheon 57922, South Korea.

Received: 18 June 2019 Accepted: 11 July 2019
Published online: 23 July 2019

References

1. Chu Q, Song K, Bu Q, Hu J, Li F, Wang J, Chen X, Shi A (2018) Two-stage pretreatment with alkaline sulphonation and steam treatment of Eucalyptus woody biomass to enhance its enzymatic digestibility for bioethanol production. Energy Convers Manag 75:236–245
2. Lei ZP, Hu ZQ, Shui HF, Ren SB, Wang ZC, Kang SG, Pan CX (2015) Pyrolysis of lignin following ionic liquid pretreatment at low temperature. Fuel Process Technol 138:612–615

3. Luo X, Mohanty A, Misra M (2013) Lignin as a reactive reinforcing filler for water-brown rapid biofoam composites from soy oil-based polyurethane. Ind Crop Prod 47:13–19
4. Asatryan R, Bennadji H, Bozzelli JW, Ruckenstein E, Khachatryan L (2017) Molecular products and fundamentally based reaction pathways in the gas-phase pyrolysis of the lignin model compound p-coumaryl alcohol. J Phys Chem A 121:3352–3371
5. Dorrestijin E, Laarhoven LJ, Arends IW, Mulder P (2000) The occurrence and reactivity of phenoxyl linkages in lignin and low rank coal. J Anal Appl Pyrolysis 54:153–192
6. Kubo S, Kadla JF (2005) Lignin-based carbon fibers: effect of synthetic polymer blending on fiber properties. J Polym Environ 13:97–105
7. Yin L, Leng E, Gong X, Zhang Y, Li X (2018) Pyrolysis mechanism of ß-O-4 type lignin model polymers with different oxygen functional groups on Cα. J Anal Appl Pyrolysis 136:169–177
8. Liu LY, Cho MJ, Sathitsuksanoh N, Chowdhury S, Renneckar S (2018) Uniform chemical functionality of technical lignin using ethylene carbonate for hydroxyethylation and subsequent greener esterification. ACS Sustain Chem Eng 6:12251–12260
9. Culebras M, Beaucamp A, Wang Y, Clauss MM, Frank E, Collins MN (2018) Biobased structurally compatible polymer blends based on lignin and thermoplastic elastomer polyurethane as carbon fiber precursors. ACS Sustain Chem Eng 6:8816–8825
10. Kai D, Zhang K, Liow SS, Loh XJ (2019) New dual functional PHB-grafted lignin copolymer: synthesis, mechanical properties, and biocompatibility studies. ACS Appl Bio Mater 2:127–134
11. Jeong HJ, Cha JY, Choi JH, Jang KS, Lim J, Kim WY, Seo DC, Jeon JR (2018) One-pot transformation of technical lignins into humic-like plant stimulants through Fenton-based advanced oxidation: accelerating natural fungus-driven humification. ACS Omega 3:7441–7453
12. Ahmad M, Rajapaksha AU, Lim JE, Zhang M, Bolan N, Mohan D, Vithanage M, Lee SS, Ok YS (2014) Biochar as a sorbent for contaminant management in soil and water: a review. Chemosphere 99:19–33
13. Guo X, Zhang S, Shan X (2008) Adsorption of metal ions on lignin. J Hazard Mater 151:134–142
14. Wu Y, Zhang S, Guo X, Huang H (2008) Adsorption of chromium(III) on lignin. Bioresour Technol 99:7709–7715
15. Ge Y, Li Z (2018) Application of lignin and its derivatives in adsorption of heavy metal ions in water: a review. ACS Sustain Chem Eng 6:7181–7192
16. da Silva LG, Ruggiero R, Gontijo PM, Pinto RB, Royer B, Lima EC, Fernandes THM, Calvete T (2011) Adsorption of Brilliant Red 2BE dye from water solutions by a chemically modified sugarcane bagasse lignin. Chem Eng J 168:620–628
17. Wang X, Jiang C, Hou B, Wang Y, Hao C, Wu J (2018) Carbon composite lignin-based adsorbents for the adsorption of dyes. Chemosphere 206:587–596
18. Tang Y, Hu T, Zeng Y, Zhou Q, Peng Y (2015) Effective adsorption of cationic dyes by lignin sulfonate polymer based on simple emulsion polymerization: isotherm and kinetic studies. RCS Adv 5:3757–3766
19. Nair V, Panigrahy A, Vinu R (2014) Development of novel chitosan-lignin composites for adsorption of dyes and metal ions from wastewater. Chem Eng J 254:491–502
20. Tan KB, Vakili M, Horri BA, Poh PE, Abdullah AZ, Salamatinia B (2015) Adsorption of dyes by nanomaterials: recent developments and adsorption mechanisms. Sep Purif Technol 150:242–292
21. Li Y, Wang Z, Xie X, Zhu J, Li R, Qin T (2017) Removal of Norfloxacin from aqueous solution by clay-biochar composite prepared from potato stem and natural attapulgite. Colloid Surf A 514:126–136
22. Chowdhury S, Mishra R, Saha P, Kushwaha P (2011) Adsorption thermodynamics, kinetics and isosteric heat of adsorption of malachite green onto chemically modified rice husk. Desalination 265:159–168
23. Ngah WSW, Md Ariff NF, Hashim A, Hanafiah MAKM (2010) Malachite green adsorption onto chitosan coated bentonite beads: isotherms, kinetics and mechanism. Clean Soil Air Water 38:394–400
24. Arellano-Cárdenas S, López-Cortez S, Cornejo-Mazón M, Mares-Gutiérrez JC (2013) Study of malachite green adsorption by organically modified clay using a batch method. Appl Surf Sci 280:74–78
25. Baek MH, Ijagbemi CO, Se-Jin O, Kim DS (2010) Removal of malachite green from aqueous solution using degreased coffee bean. J Hazard Mater 176:820–828
26. Hameed BH, El-Khaiary MI (2008) Batch removal of malachite green from aqueous solutions by adsorption on oil palm trunk fibre: equilibrium isotherms and kinetic studies. J Hazard Mater 154:237–244
27. Hameed BH, El-Khaiary MI (2008) Malachite green adsorption by rattan sawdust: isotherm, kinetic and mechanism modeling. J Hazard Mater 159:574–579
28. Bulut E, Özacar M, Şengil IA (2008) Adsorption of malachite green onto bentonite: equilibrium and kinetic studies and process design. Microporous Mesoporous Mater 115:234–246
29. Saha P, Chowdhury S, Gupta S, Kumar I (2010) Insight into adsorption equilibrium, kinetics and thermodynamics of malachite green onto clayey soil of India origin. Chem Eng J 165:874–882
30. Han R, Wang Y, Sun Q, Wang L, Song J, He X, Dou C (2010) Malachite green adsorption onto natural zeolite and reuse by microwave irradiation. J Hazard Mater 175:1056–1061
31. Vasanth Kumar K, Sivanesan S, Ramamurthi V (2005) Adsorption of malachite green onto *Pithophora* sp. a fresh water algae: equilibrium and kinetic modelling. Process Biochem 40:2865–2872
32. Zhang J, Li Y, Zhang C, Jing Y (2008) Adsorption of malachite green from aqueous solution onto carbon prepared from Arundo donax root. J Hazard Mater 150:774–782
33. Hameed BH, El-Khaiary MI (2008) Equilibrium, kinetic and mechanism of malachite green adsorption on activated carbon prepared from bamboo by K_2CO_3 activation and subsequent gasification with CO_2. J Hazard Mater 157:344–351
34. Rahman IA, Saad B, Shaidan S, Sya Rizal ES (2005) Adsorption characteristics of malachite green on activated carbon derived from rice husks produced by chemical-thermal process. Bioresour Technol 96:1578–1583
35. Ahmad R, Kumar R (2010) Adsorption studies of hazardous malachite green onto treated ginger waste. J Environ Manag 91:1032–1038
36. Malik R, Ramteke DS, Wate SR (2007) Adsorption of malachite green on groundnut shell waste based powdered activated carbon. Waste Manag 27:1129–1138
37. Önal Y, Akmil-Başar C, Sarıcı-Özdemir Ç (2007) Investigation kinetics mechanisms of adsorption malachite green onto activated carbon. J Hazard Mater 146:194–203
38. Boutsika LG, Karapanagioti HK, Manariotis ID (2014) Aqueous mercury sorption by biochar from malt spent rootlets. Water Air Soil Pollut 225:1805
39. Tan G, Sun W, Xu Y, Wang H, Xu N (2016) Sorption of mercury(II) and atrazine by biochar, modified biochars and biochar based activated carbon in aqueous solution. Bioresour Technol 211:727–735
40. Inyang M, Gao B, Zimmerman A, Zhang M, Chen H (2014) Synthesis, characterization, and dye sorption ability of carbon nanotube-biochar nanocomposites. Chem Eng J 236:39–46
41. Arias FEA, Beneduci A, Chidichimo F, Furia E, Straface S (2017) Study of the adsorption of mercury(II) on lignocellulosic materials under static and dynamic conditions. Chemosphere 180:11–23
42. Leng L, Yuan X, Zeng G, Shao J, Chen X, Wu Z, Wang H, Peng X (2015) Surface characterization of rice husk bio-char produced by liquefaction and application for cationic dye (Malachite green) adsorption. Fuel 155:77–85
43. Harmita H, Karthikeyan KG, Pan X (2009) Copper and cadmium sorption onto kraft and organosolv lignins. Bioresour Technol 100:6183–6191
44. Gűrses A, Doğar Ç, Yalçın M, Açıkyıldız M, Bayrak R, Karaca S (2006) The adsorption kinetics of the cationic dye, methylene blue, onto clay. J Hazard Mater B131:217–228
45. Bhattacharyya KG, Gupta SS (2006) Kaolinite, montmorillonite, and their modified derivatives as adsorbents for removal of Cu(II) from aqueous solution. Sep Purif Technol 50:388–397
46. Badruddoza AZM, Hazel GSS, Hidajat K, Uddin MS (2010) Synthesis of carboxymethyl-β-cyclodextrin conjugated magnetic nano-adsorbent for removal of methylene blue. Colloids Surf A 367:85–95
47. Afkhami A, Saber-Tehrani M, Bagheri H (2010) Modified maghemite nanoparticles as an efficient adsorbent for removing some cationic dye from aqueous solution. Desalination 263:240–248
48. Barford JP, Mckay G (2009) Reactive Black dye adsorption/desorption onto different adsorbents: effect of salt, surface chemistry, pore size and surface area. J Colloid Interface Sci 337:32–38
49. Keiluweit M, Nico PS, Johnson MG, Kleber M (2010) Dynamic molecular structure of plant biomass-derived black carbon (biochar). Environ Sci Technol 44:1247–1253

50. El Mansouri NE, Salvadó J (2007) Analytical methods for determining functional groups in various technical lignins. Ind Crop Prod 26:116–124
51. Bekçi Z, Seki Y, Cavas L (2009) Removal of malachite green by using an invasive marine alga *Caulerpa racemose var. cylindracea*. J Hazard Mater 161:1454–1460
52. Park JH, Wang JJ, Kim SH, Cho JS, Kang SW, Delaune RD, Han KJ, Seo DC (2017) Recycling of rice straw through pyrolysis and its adsorption behaviors for Cu and Zn ions in aqueous solution. Colloids Surf A 533:330–337
53. Ahmad M, Lee SS, Dou X, Mohan D, Sung JK, Yang JE, Ok YS (2012) Effects of pyrolysis temperature on soybean stover- and peanut shell-derived biochar properties and TCE adsorption in water. Bioresour Technol 118:536–544
54. Das DD, Schnitzer MI, Monreal CM, Mayer P (2009) Chemical composition of acid–base fractions separated from bio-oil derived by fast pyrolysis of chicken manure. Bioresour Technol 100:6524–6532

Publisher's Note